6

Characteristics of Abrasive Particles and Their Implications on Wear

Giuseppe Pintaude
Federal University of Technology – Paraná
Brazil

1. Introduction

Geometry, hardness and size can be considered the most important characteristics affecting the wear rate caused by abrasive particles. The combined effect of these characteristics on wear has not yet been modeled as a whole. One particular model, proposed by Rabinowicz et al. (1961), involves a single particle being considered as a pointed tool, so that the effect of the geometry can be determined.

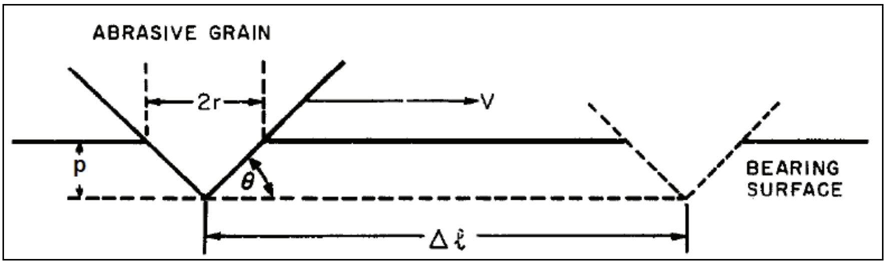

Fig. 1. Conical abrasive particle cutting a groove of depth *p*, and sliding for a distance Δl to produce a wear volume *V* (Rabinowicz et al., 1961).

The wear rate is expressed as follows:

$$dV / dl = \frac{tan\theta}{\pi}\frac{W}{H} \quad (1)$$

where $tan\theta$ is the average tangents of all roughness angles of the abrasive particles, *H* is the hardness of bearing surface and *W* is the total load.
In this case the particle is considered to be a solid body that neither degrades nor changes size and whose properties remain constant throughout the whole wear process. This hypothesis is not verified, especially for those situations where the hardness of abrasive is lower than the abraded material. This situation led to small wear rates, and it is usually classified as mild wear (Gates, 1998). The fragmentation of particles depends on their fracture toughness, and it is possible to verify in the literature data that the higher the hardness, the higher the fracture toughness (Fig. 2). Therefore, for softer abrasives the breakage is easier.

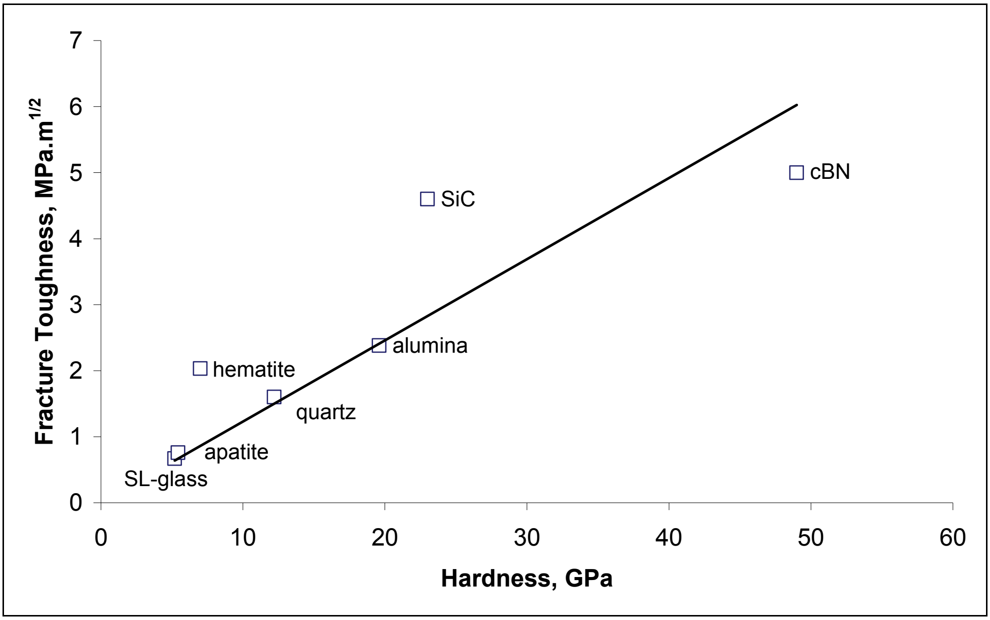

Fig. 2. Hardness and fracture toughness for usual abrasive materials. Data from Broz et al. (2006) for apatite, quartz and alumina; Rhee et al. (2001) for glass; Kaur et al. (2009) for SiC; Taniguchi et al. (1996) for cBN, and Tromans & Meech (2002) and Beste & Jacobson (2003) for hematite.

A likely effect of fragmentation is the reduction of size, another important characteristic of abrasive not incorporated in (1) (Rabinowicz et al., 1961). The well-known effect of particle size in wear rates was studied by Coronado & Sinatora (2009) for mottled cast iron with different contents of retained austenite (Fig. 3).

From Fig. 3 a high increase of mass loss with abrasive size can be observed, up to approximately 70 microns. After this, the mass losses do not increase at the same rate, and even in some cases, they do not change from a critical particle size. Many theories have been proposed to explain the effect of particle size in abrasive wear (Misra & Finnie, 1981), but a particularly important model, proposed by Sin et al. (1979) related this behavior to the abrasive characteristic considered by Rabinowicz et al. (1961): the particle geometry.

Sin et al. (1979) assumed that the abrasive particles are conical in shape with a hemispheric tip. With this hypothesis, they explained the effect of particle size on wear rates due to the changes in the tip radius. Therefore, the smaller the particle, the higher the tip radius, i.e., the small particles have rounder tips, and one can assume that they abrade a surface in the same manner of spherical particles.

Although this theory was criticized by Misra & Finnie (1981), there are many experimental evidences that support it. A good aim is to design the particle geometry that reproduces the practical results. For example, three numerical simulations (Jacobson et al., 1988, Jiang et al., 1998 and Fang et al., 2009) assumed the same geometry adopted by Sin et al. (1979) for the abrasive particles. In all cited investigations the particle size effect was very well-reproduced. Besides these studies, two experimental evidences can be mentioned also.

Firstly, Graham & Baul (1972) obtained for an aluminum alloy tested in a single pass scratch the results shown in Fig. 4.

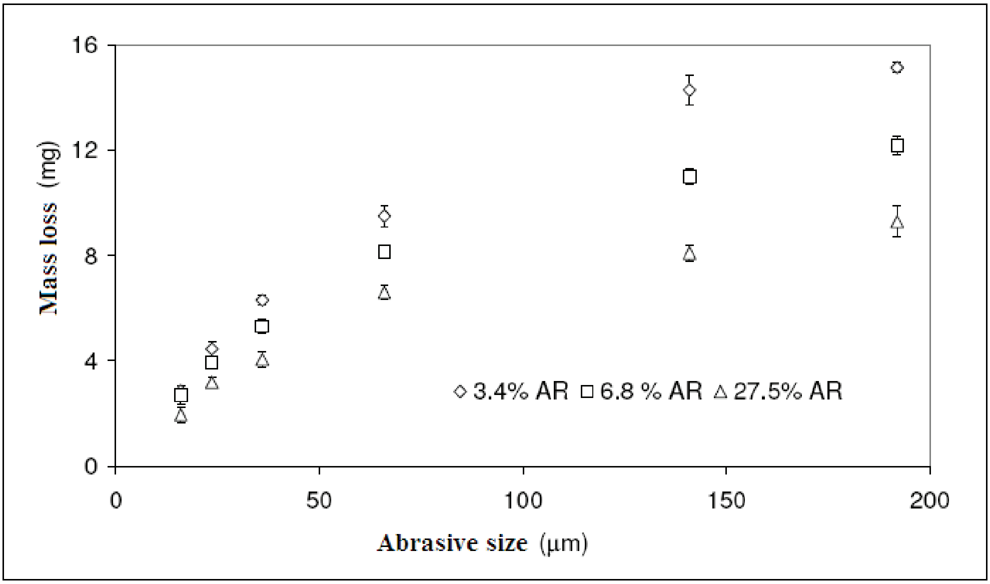

Fig. 3. Effect of abrasive size on mass loss of mottled cast iron with different retained austenite contents (Coronado & Sinatora, 2009).

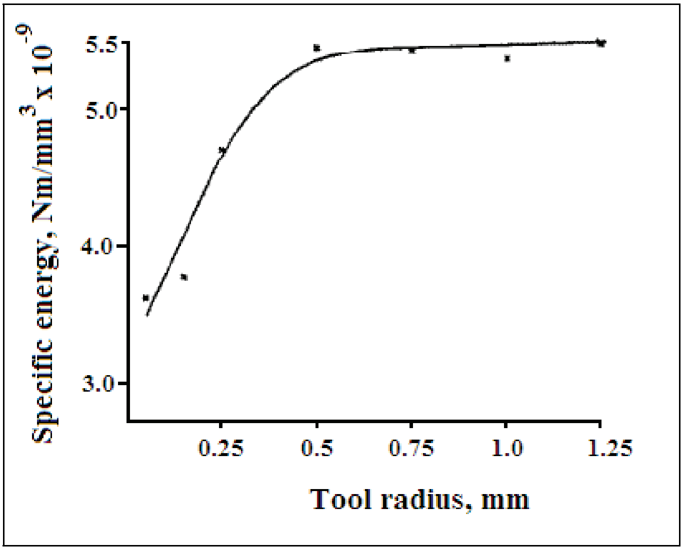

Fig. 4. Specific energy of cutting as a function of tool radius of spherical tip tool on the apex of a 90° cone (Graham & Baul, 1972).

Although these results are expressed in terms of specific energy as a function of tool radius, they can be correlated with results as those presented in Fig. 3. In the scratch test an increase in the tool radius means that the aluminum alloy experienced a contact with a blunt tool. Following Sin et al. (1979), small particles behave like blunt ones. In addition, the specific energy for cutting is high for small particles, as demonstrated in some investigations (Jacobson et al., 1988, Jiang et al., 1998).

The second example favorable to the bluntness theory was given by Gahlin & Jacobsson (1999). They produced controlled surfaces using micro mechanical etching technique, and different particle sizes were simulated by changing the packing density. Their main results are presented in Fig. 5, having tin as the worn material.

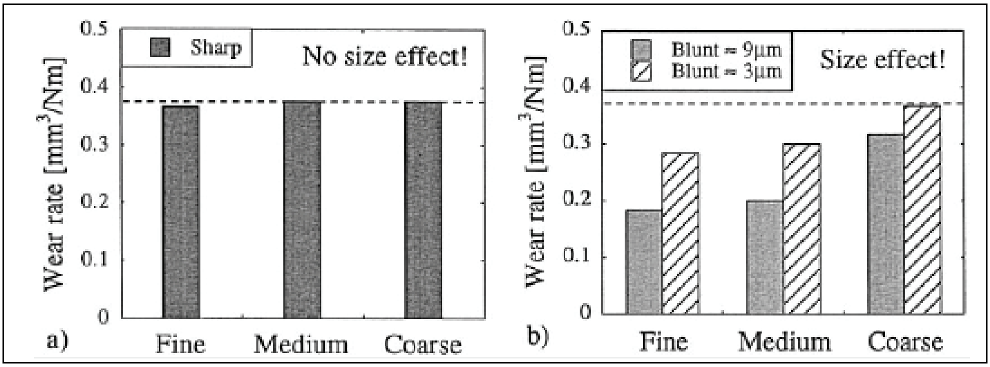

Fig. 5. The wear rate varying with packing density, considering: (a) sharp and (b) blunt tips (Gahlin & Jacobsson, 1999).

Fig. 5a shows that the size effect was not observed for the sharp tips. On the other hand, blunt tips exhibited a significant size effect. These results thus confirm that the relative bluntness theory is able to explain the effect of abrasive size in wear rates.

In the next item we will discuss possible approaches to characterize the abrasive wear, considering the difficulty to determine the level in which a particle loses its sharpness and the strong relationship between this and the mechanical properties of abrasive, such as hardness and fracture toughness, as previously described.

2. Approaches to characterize abrasive wear

Fig. 6 presents a sequence of events since a particle abrading a surface to the material removal step, resulting in a production of debris.

The wear debris characterization is still little employed in abrasion process (Stachowiak et al., 2008), so that this aspect will be not treated here.

The first approach to characterize the abrasive wear process can be made through the shape evaluation of abrasive particles. There are a lot of shape parameters, including the aspect ratio, roundness and fractal dimension (Kaye, 1998). Special attention to new developments to shape evaluation is given by Stachowiak and co-workers in a series of investigations. A remarkable definition is the spike parameter – quadratic fitting (SPQ) (Hamblin and Stachowiak, 1996), which is based on the localization of the centroid of the bi-dimensional section of particle and the circle in which radius is equal to the average radius

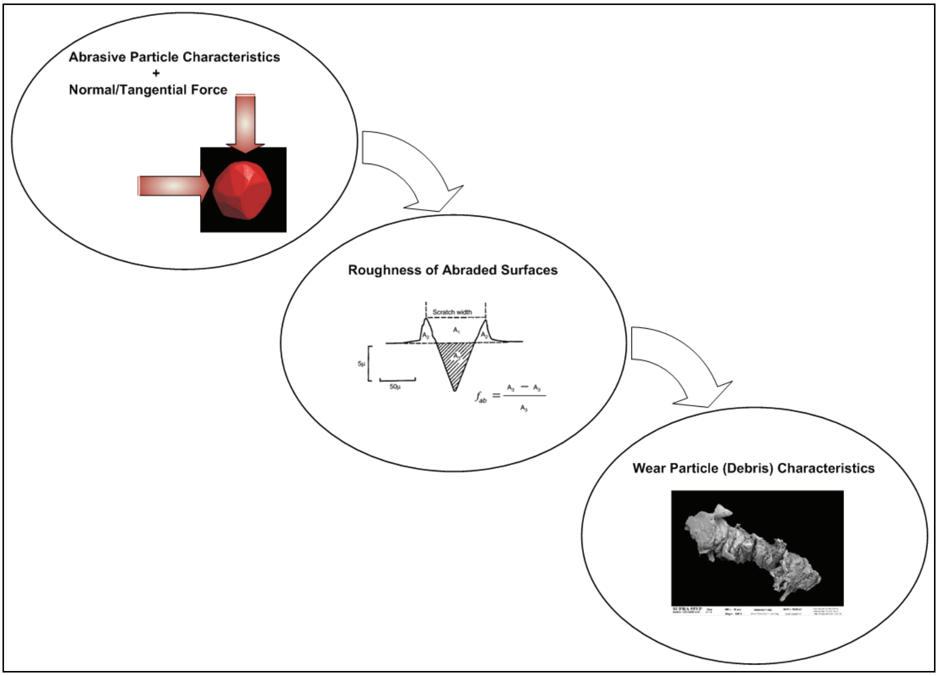

Fig. 6. Three ways to characterize the abrasive wear. Images adapted from De Pellegrin & Stachowiak (2005), Buttery & Archard (1971) and Stachowiak et al. (2008).

of particle (Fig. 7). The areas outside the circle are considered as interest regions, whereas the bulk is suppressed. The maximum local diameter is determined for each region outside the circle and this point is treated as spike vertices, M. The spike laterals, which are between the segments sp-mp and mp-ep are represented by polynomial quadratic functions. Differentiating the functions at point mp, led in the apex angle θ .

$$sv = \cos(\theta / 2) \quad (2)$$

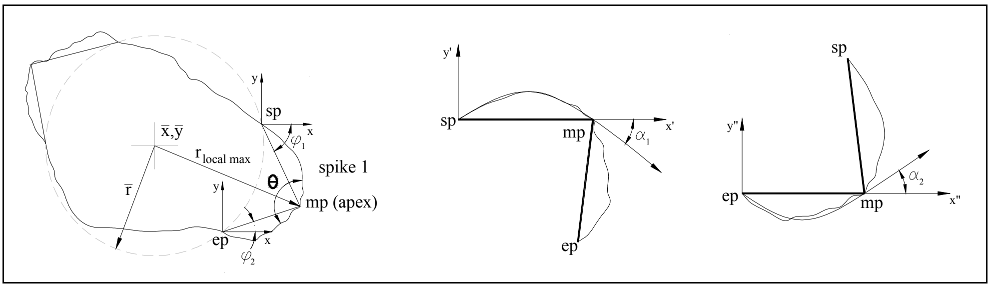

Fig. 7. Routine to calculate the spike parameter SPQ.

The spike parameter – quadratic fitting (SPQ) is thus obtained from the average value of valid spikes, where n is the number of found spikes:

$$SPQ = \frac{1}{n}\sum sv \tag{3}$$

The second possible form to characterize the abrasion process is to measure the surface roughness of an abraded material. Spurr (1981) proposed that the ploughing contribution to friction can be related to the roughness parameters, as follows:

$$\mu_P = \frac{8}{\pi}\frac{Ra}{\lambda a} \tag{4}$$

Taken into account the definition of $\lambda a\,(= 2\pi\, Ra / \Delta a)$, (4) can be rewritten as

$$\mu_P \cong 0.4\ \Delta a \tag{5}$$

where Δa is defined as the mean absolute profile slope over the assessment length.
Torrance (2002) defined the parameter Rqs as the rms slope of abrasive in contact with abraded material. In his description, both wear and friction coefficients are depended on this parameter. A simple definition provided by Torrance for this parameter is:

$$Rqs = p\sqrt{\frac{H_S}{f_n}} \tag{6}$$

where f_n is the normal force per grit, H_S is the surface hardness of metal, and p is the average scratch depth made by abrasives. If the geometry of abrasive was perfectly transferred to the worn surface, it would be possible to associate the Torrance's definition to the rms slope of the profile, Δq .

More recently, Da Silva & De Mello (2009) used the hybrid bi-dimensional parameter $\lambda q\,(= 2\pi\, Rq / \Delta q)$, which represents the root mean square wavelength of the profile, and considering that this parameter can be associated to the width of the scratches, they found a relationship between scratch widths and normal load using the single scratch experiments.
All definitions above mentioned made use of a roughness parameter of height and another that express the slope. The relationship between each other can be a good indicative of the contact area between abrasive and abraded surface. For example, McCool (1987) proposed an easily programmed method using the rms height and rms slope to estimate the contact area in a microcontact model.

3. Experimental

The wear and friction coefficients were presented elsewhere in Pintaude et al. (2003) and Pintaude et al. (2009), in tests performed under sliding abrasion using pin-on-disk apparatus. The tested materials were obtained from three groups:

- Low-carbon steel (composition similar to AISI 1006 steel).
- Bearing wiredrawn steel (AISI 52100).
- High-chromium cast iron.

The low-carbon steel was tested in the as-cast condition. The bearing steel (Q&T 52100 steel) and the high-chromium cast iron (HCCI) were heat-treated. The Vickers hardness of tested materials is presented in Table 1.

Material	HV_1, MPa
Low-carbon steel (1006 steel)	973
Bearing steel (Q&T 52100 steel)	4070
High-chromium cast iron (HCCI)	4600

Table 1. Vickers hardness of tested materials.

Pins of 3 mm diameter and 21 mm length were tested in a pin-on-disk apparatus, using abrasive papers coated disks. Conditioning of the pin surface before starting the test was made using a grit 600 corundum paper. The abrasives used in the tests were glass paper, either with 80 grit (0.20 mm average grain size) or 240 grit (0.06 mm of average grain size).

During tests the following variables were controlled: rotational and tangential velocities, number of revolutions, position of the pin in relation to the disc, sliding distance, tangential and normal forces, friction coefficient, room relative humidity and room temperature.

All tests were performed using 20 N of normal force, applied by deadweight. At least seven mass determinations were made for each test piece.

An analytical scale with 0.1 mg resolution was used to measure pin mass. A minimum mass variation of 1 mg was established for each test, in order to avoid the error of scale. In the case of the more wear resistant test pieces, up to 10 abrasive papers were used for each test.

With the measurement of mass losses and friction coefficients, it is possible to calculate the abrasion factor, f_{ab}, defined as the proportion of groove volume removed. The volume of material displaced is equal to the area A3 but, of this material, a volume equal to the area A2 is retained upon the surface as piled-up material. Thus, the volume of material removed (wear) is equal to (A3-A2) (see Fig. 8). An alternative used to determine f_{ab} is presented by Jacobson et al. (1988), defined in (7):

$$f_{ab} = K_A / \mu_P \quad (7)$$

where K_A is the wear coefficient and μ_P is the ploughing component of the friction coefficient. To find μ_P, the adhesive component of the friction coefficient is assumed as 0.2, so that this value is reduced from the whole friction coefficient values provided by Pintaude et al. (2003, 2009).

After the wear tests, the surface roughness of worn pins was determined, using 1.75 mm as sampling length, performed in PERTHOMETER v 6.2 equipment. The calculations of roughness parameters were made using MATLAB 5® software, 5.3 version. In this software, two filters were applied: one to remove the waviness of profile and another one to determine the mean line. After that, the profiles were divided into 7 cut-offs, of which the initial and final were discarded, and the remaining 5 were used to obtain the roughness parameters values. The routine of calculation was adequately tested in a standard block supplied with the roughness measuring equipment.

The glass particles were extracted from papers to analyze their shape factors. Twenty particles were randomly selected from two samples of glass, whose average size are 72 and 455 microns. These particles were removed from papers of #80 and #240 mesh, respectively. The images obtained in optical microscope were then submitted to threshold process in the Image-Pro Plus software to convert the grayscale to binary image (Fig. 9). The output binary images has values of 1 (white) for all pixels in the input image with luminance greater than defined level and 0 (black) for all other pixels. The transition level was based on the histogram of images. The Image-Pro Plus software has routines to calculate the average values of roundness factor, fractal dimension and aspect ratio and these shape factors were determined for each group of glass particles.

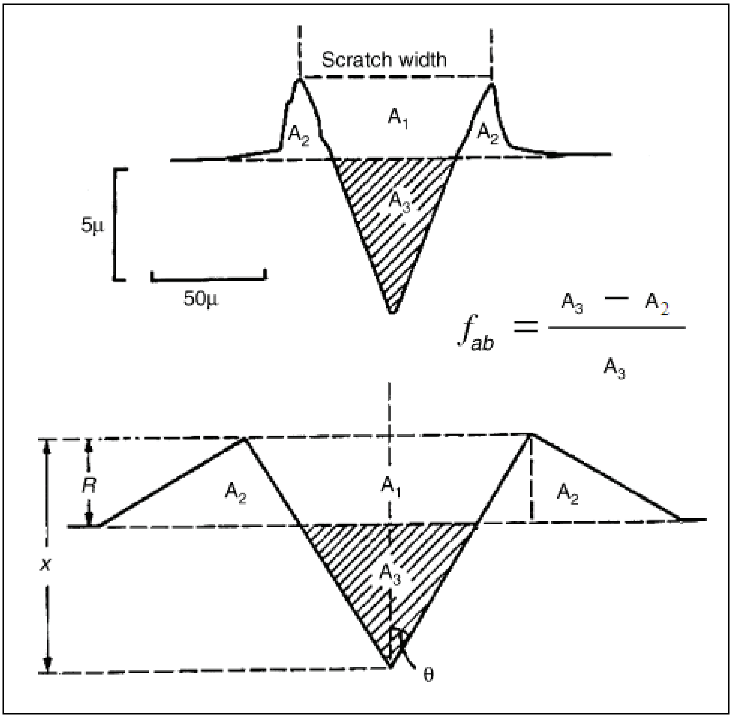

Fig. 8. Abrasion factor definition (Buttery & Archard, 1971).

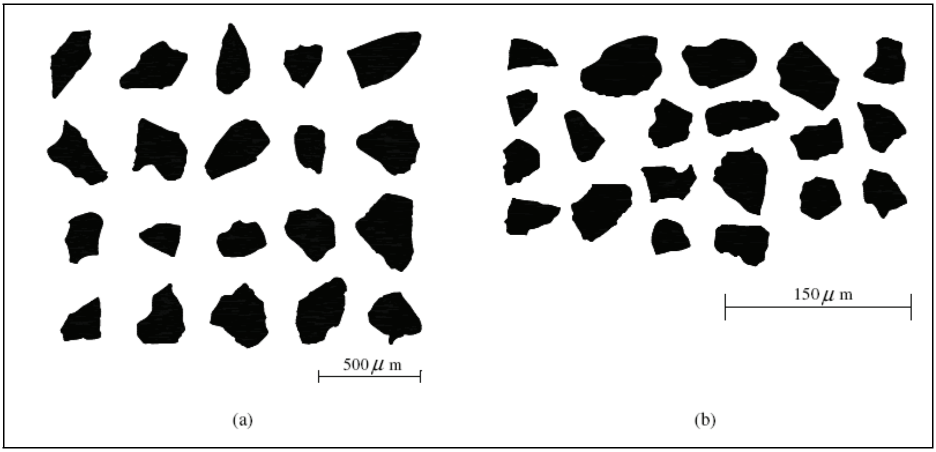

Fig. 9. Binary images of glass particles: (a) 72 microns and (b) 455 microns average size.

4. Results and discussion

Table 2 shows the shape factors determined for glass particles removed from #80 and #240 papers. Also, the wear rates promoted by these particles abrading quenched and tempered 52100 steel with 4.07 GPa Vickers hardness after sliding abrasion tests are provided.

Average size, microns	Wear rate (m^3/m)	Aspect ratio	1/Roundness	Fractal dimension
72	7.25E-12	1.5 ± 0.3	1.4 ± 0.1	1.06 ± 0.01
455	6.84E-11	1.5 ± 0.3	1.5 ± 0.1	1.07 ± 0.01

Table 2. Shape factors values for different glass particle sizes and the respective wear rates of 52100 steel caused by them

The wear rates were very much affected by the glass particle size. The increase from 72 to 455 microns caused an increase of one order of magnitude in wear rates. The values of shape factors presented in Table 2 do not corroborate the theory given by Sin et al. (1979), since there is no difference among them.

The insignificant effect of average size on shape factor was also demonstrated by Bozzi & De Mello (1999). When they tested silica grains against WC-12%Co thermal sprayed coating in three-body abrasion during 330 min, the average size of abrasive particles were reduced in 38.2%. This reduction did not occur in the same proportion for the roundness factor: only 2.9% of reduction was observed for the shape value. An important aspect of tests performed by Pintaude et al. (2009) and Bozzi & De Mello (1999) is that the hardness of abrasive is lower than that of worn material, resulting in a mild wear. In these cases, a possible explanation for the failure of a particle to penetrate another surface is that the geometry of the particle that is not sufficiently hard to produce a scratch on the other material must have undergone a change after its breakage. The particles indeed break, as has been shown in an earlier study (Pintaude et al., 2003). Thus, instead of having more points to cut with, the broken particle ends up becoming blunter, so that it cannot cut. However, the shape characterization did not prove this.

Another set of results was obtained by De Pellegrin & Stachowiak (2002) (Fig. 10), broader than those presented in Table 2 and by Bozzi & De Mello (1999). Again, no one can observe any variation of the shape factor (aspect ratio) with particle size.

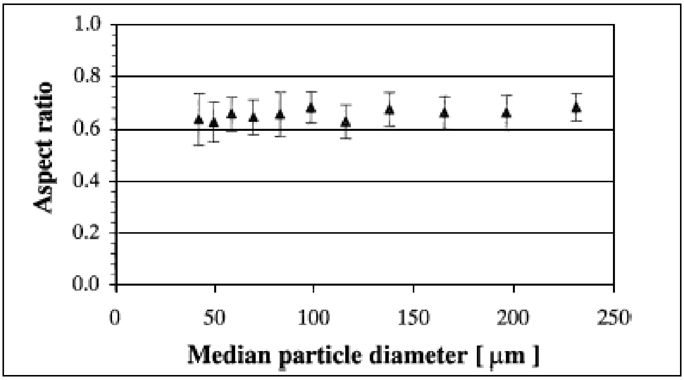

Fig. 10. Aspect ratio of alumina particles as a function of their median particle diameter (De Pellegrin & Stachowiak, 2002).

Although the presented results had been contrary to the bluntness theory, the same cannot be discharged due to an important reason. The shape factors determination should be considered as a bi-dimensional analysis and the action of abrasive during mechanical contact occurred in 3D dimension. Thus, De Pellegrin & Stachowiak (2002) pointed out that the presence of re-entrant features made a difference between the induced groove area and the calculated one from the particle projection. For this reason, we will test now some ideas about roughness characterization of abraded surfaces.

Table 3 presents the results of abrasion factors for 1006 and 52100 steels and for high-chromium cast iron abraded by glass papers. In addition, the root mean square wavelength values of abraded surfaces were also presented.

	λq , mm		f_{ab} ($\equiv K_A/\mu_P$)	
Worn material	#80 paper	#240 paper	#80 paper	#240 paper
1006 steel	23.2	16.3	0.0411	0.021
Q&T 52100 steel	39	26.9	0.106	0.037
HCCI	26.6	N.T.	0.00895	N.T.

Table 3. The root mean square wavelength of the profile and the estimated abrasion factor of three materials tested in sliding abrasion using glass as abrasive. N.T.: not tested.

The results presented in Table 3 show expected trends for steels, abraded in severe wear: the abrasion factor is higher for the hardest steel and lower as the abrasive particle size is reduced. In addition, the volume removed as debris to volume of micro-grooves of pins in repeated sliding determined by Hisakado et al. (1999) was in the same order of magnitude of those presented in Table 3 for tested steels.

Now, it is important to establish a possible relationship between the λq and f_{ab} values. Taken into account the results obtained for 1006 steel tested with #80 paper and for 52100 steel abraded by #240 glass particles one can conclude that the abrasion factors were similar, and at the same time, as well as the λq ones. Again, it is remarkable that the wear in these cases was severe, i.e., the hardness of abrasive is higher than the hardness of steels.

An important observation from λq results is that these values are more affected by Rq than the Δq values, i.e., the increase in particle size leads to an increase in the height profile, and the slope kept almost unmodified. This kind of result was already described by Hisakado & Suda (1999) in abrasive papers, when they measured the slope of SiC particles with different grain sizes (Table 4).

Abrasive papers	Average size, microns	Slope angle of abrasive grain	Rms roughness, microns
#100	125	47.2	68.2
#1000	16.3	54.1	10.7

Table 4. Topographical properties measured on abrasive papers constituted of SiC particles (Hisakado & Suda, 1999).

In order to reinforce the above discussion, a scheme given by Gahlin & Jacobson (1999) (Fig. 11) shows how the increase of particle size can mean a change only in the height roughness parameter with no variation in the slope of surface. In Fig. 11, D3 > D2 > D1, being D the diameter of particle, and H3 > H1, being H the total height imprint at surface.

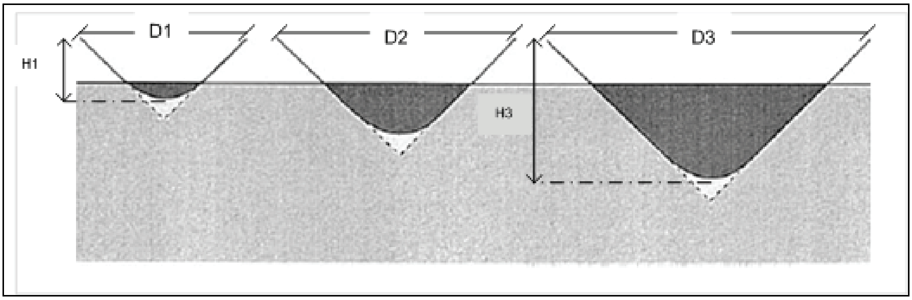

Fig. 11. Illustration showing a simultaneously increase of particle diameter and total height (adapted from Gahlin & Jacobson, 1999).

From the above analysis, we can conclude that the λq roughness parameter is a powerful variable to characterize an abraded surface, discriminating the effect of particle size under severe wear. In this situation, the abrasive characteristics are changed a little during the mechanical contact.

On the other hand, a very different situation occurred for HCCI. At present, this material was abraded under mild wear, and a severe fragmentation of glass particles was observed. The f_{ab} is very lower than that observed for 52100 steel (Tab. 3), despite the fact that their difference in hardness is not significant. In addition, any kind of correlation is possible to make with the λq value, as made for the steels between λq and f_{ab}.

Here, we identified a lack in the literature proposals to identify changes that happens during the contact between a soft abrasive and a hard abraded surface, even the bluntness theory proposed by Sin et al. (1979) has received good experimental evidences, as previously discussed.

We pay heed to other evidence in the literature to support it, since the relationship between static hardness tests and abrasion is always employed. Following the definitions provided by Buttery & Archard (1971) (Fig. 8), the fraction of material displaced is reduced as the severity of pile-up increases. The surface deformation, after the complete unloading, was evaluated by Alcalá et al. (2000) for spherical and Vickers geometry indenters, considering the static indentation process. The results obtained by these researches for work-hardened copper is presented in Fig. 12.

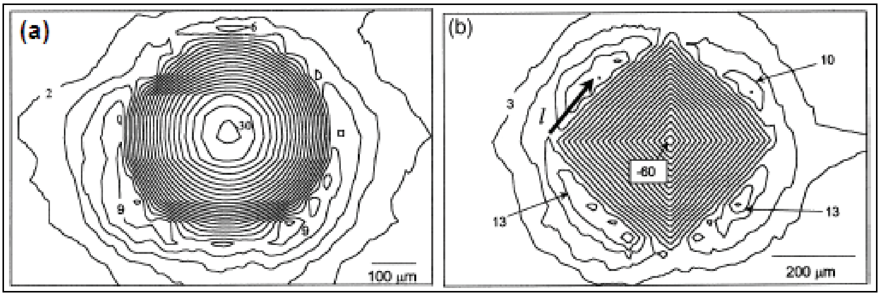

Fig. 12. Surface topography around spherical (a) and Vickers (b) indents for an indentation load of 160 N performed in a work-hardened copper. The dimensions are provided in microns (Alcalá et al., 2000).

The height dimensions at the center of indentation and at its ridges allow calculating the severity of pile-up (s), following (8). Thus, one can conclude that the spherical indentation gives rise to a larger severity of pile-up. It implies that f_{ab} produced by a spherical indenter should be smaller than that estimated for a pyramidal (angular). The small particles tested by Pintaude et al. (2009) produced low values of f_{ab}, confirming the possibility that they scratch the surface as spherical particles.

$$s = \frac{R}{x} \tag{8}$$

5. Conclusions and future trends

The measurement of shape factors using bi-dimensional technique is not useful to prove the theory put forward by Sin et al. (1979) used to explain the particle size effect in abrasive wear rates, although a series of experimental evidences support it. The main reason for this discrepancy is the 3D action of abrasives during the wear process, and a bi-dimensional characterization probably disregards the presence of re-entrant features of particles in this case.

For severe abrasion, when the hardness of abrasive is higher than the worn surface material, the use of roughness characterization by means of a hybrid parameter is a good way to discriminate the particle size effect, probably due to the undermost changes in the slope of particles, which have a high cutting capacity providing by a combination of their hardness and fracture toughness.

However, for mild abrasion, when the level of particles breakage is high, the surface characterization presented here is not yet enough to discriminate the size effects. Therefore, as a future trend we indicate the development of analytical tools able to detect the changes in abrasive sizes after their breakage, and the measurement of consequences of this process in their geometries.

6. References

Alcalá, J., Barone, A.C. & Anglada, M. (2000). The influence of plastic hardening on surface deformation modes around Vickers and spherical indents, *Acta Materialia*, Vol. 48, No. 13, pp. 3451-3464, ISSN: 1359-6454.

Beste, U. & Jacobson, S. (2003). Micro scale hardness distribution of rock types related to rock drill wear, *Wear*, Vol. 254, No. 11, pp. 1147-1154, ISSN: 0043-1648.

Bozzi, A.C. & De Mello, J.D.B. (1999). Wear resistance and wear mechanisms of WC–12%Co thermal sprayed coatings in three-body abrasion. *Wear*, Vol. 233–235, December, pp. 575–587.

Broz, M.E., Cook, R.F. & Whitney, D.L. (2006). Microhardness, Toughness, and Modulus of Mohs Scale Minerals, *American Mineralogist*, Vol. 91, No. 1, pp. 135–142, ISSN: 0003-004x.

Buttery, T.C. & Archard, J.F. (1970). Grinding and abrasive wear. *Proc. Inst. Mech. Eng.*, Vol. 185, pp. 537-552, ISSN: 0020-3483.

Coronado, J.J. & Sinatora, A. (2009). Particle size effect on abrasion resistance of mottled cast iron with different retained austenite contents, Wear, Vol. 267, No. 1-4, pp. 2077-2082.

Da Silva, W.M. & De Mello, J.D.B. (2009). Using parallel scratches to simulate abrasive wear. *Wear*, Vol. 267, No. 11, pp. 1987–1997.
De Pellegrin, D.V. & Stachowiak, G.W. (2005). Simulation of three-dimensional abrasive particles. *Wear*, Vol. 258, No. 1-4, pp. 208-216.
De Pellegrin, D.V. & Stachowiak, G.W. (2002). Assessing the role of particle shape and scale in abrasion using 'sharpness analysis' Part II. Technique evaluation. *Wear*, Vol. 253, No. 9-10, pp. 1026–1034.
Fang, L., Li, B., Zhao, J. & Sun, K. (2009). Computer simulation of the two-body abrasion process modeling the particle as a paraboloid of revolution. *Journal of Materials Processing Technology*, Vol. 209, No. 20, pp. 6124–6133, ISSN: 0924-0136.
Gahlin, R. & Jacobson, S. (1999). The particle size effect in abrasion studied by controlled abrasive surfaces. *Wear*, Vol. 224, No. 1, pp. 118-125.
Gates, J.D. (1998). Two-body and three-body abrasion: A critical discussion. *Wear*, Vol. 214, No. 1, pp. 139-146.
Graham, D. & Baul, R. M. (1972). An investigation into the mode of metal removal in the grinding process, *Wear*, Vol. 19, No. 3, pp. 301-314.
Hamblin, M.G. & Stachowiak, G.W. (1996). Description of abrasive particle shape and its relation to two-body abrasive wear. *Tribology Transactions*, Vol. 39, No. 4, pp. 803-810, ISSN: 1040-2004.
Hisakado, T. & Suda, H. (1999). Effects of asperity shape and summit height distributions on friction and wear characteristics. Wear, Vol. 225–229, Part 1, April, pp. 450–457.
Hisakado, T.; Tanaka, T. & Suda, H. (1999). Effect of abrasive particle size on fraction of debris removed from plowing volume in abrasive wear. *Wear*, Vol. 236, No. 1-2, December, pp. 24–33.
Jacobson, S., Wallen, P. & Hogmark, S. (1988). Fundamental aspects of abrasive wear studied by a new numerical simulation model. *Wear*, Vol. 123, No. 2, pp. 207-223.
Jiang, J., Sheng, F. & Ren, F. (1998). Modelling of two-body abrasive wear under multiple contact conditions. *Wear*, Vol. 217, No. 1, pp. 35-45.
Kaye, B.H. (1998). Particle shape characterization, In: *ASM Handbook Vol. 7 Powder Metal Technologies and Applications*, Lee, P.W. et al. (Ed.), 605-618, ASM International, ISBN 0-87170-387-4, Metals Park, OH
Kaur, S., Cutler, R.A. & Shetty, D.K. (2009). Short-Crack Fracture Toughness of Silicon Carbide. *J. Am. Ceram. Soc.*, Vol. 92, No. 1, pp. 179–185, ISSN: 1551-2916.
McCool, J.I. (1987). Relating profile instrument measurements to the functional performance of rough surfaces. *Journal of Tribology ASME*, Vol. 109, No. 2, pp. 264-270, ISSN: 0742-4787.
Misra, A. & Finnie, I. (1981). On the size effect in abrasive and erosive wear *Wear*, Vol. 65, No. 3, January, pp. 359-373.
Pintaude, G., Bernardes, F.G., Santos, M.M., Sinatora, A. & Albertin, E. (2009). Mild and severe wear of steels and cast irons in sliding abrasion. *Wear*, Vol. 267, No. 1-4, pp. 19-25.
Pintaude, G., Tanaka, D.K. & Sinatora, A. (2003). The effects of abrasive particle size on the sliding friction coefficient of steel using a spiral pin-on-disk apparatus. *Wear*, Vol. 255, No. 1-6, August-September, pp. 55-59.
Rabinowicz, E.; Dunn, L. A. & P. G. Russel, P.G. (1961). A study of abrasive wear under three-body conditions, *Wear,* Vol. 4, No. 5, pp. 345 - 355.

Rhee, Y-W., Kim, H-W., Deng, Y. & Lawn, B.R. (2001). Brittle fracture versus quasi plasticity in ceramics: a simple predictive index, *J. Am. Ceramic Soc.*, Vol. 84, No. 3, pp. 561-565.

Sin, H., Saka, N. & Suh, N.P. (1979). Abrasive wear mechanisms and the grit size effect. *Wear*, Vol. 55, No. 1, July, pp. 163-190.

Spurr, R.T. (1981). The abrasive wear of metals. *Wear*, Vol. 65, No. 3, pp. 315–324.

Stachowiak, G.P., Stachowiak, G.W. & Podsiadlo, P. (2008). Automated classification of wear particles based on their surface texture and shape features. *Tribology International*, Vol. 41, No. 1, January, pp. 34–43, ISSN: 0301-679X.

Taniguchi, T., Minoru Akaishi, M. & Yamaoka, S. (1996). Mechanical Properties of Polycrystalline Translucent Cubic Boron Nitride as Characterized by the Vickers Indentation Method. *J. Am. Ceramic Soc.*, Vol. 79, No. 2, pp. 547-549.

Torrance, A.A. (2002). The effect of grit size and asperity blunting on abrasive wear. *Wear*, Vol. 253, No. 7-8, pp. 813–819.

Tromans, D. & Meech, J.A. (2002). Fracture toughness and surface energies of minerals: theoretical estimates for oxides, sulphides, silicates and halides. *Minerals Engineering*, Vol. 15, No. 12, pp. 1027–1041, ISSN: 0892-6875.

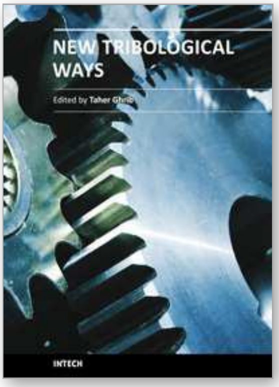

InTech Europe
University Campus STeP Ri
Slavka Krautzeka 83/A
51000 Rijeka, Croatia
Phone: +385 (51) 770 447
Fax: +385 (51) 686 166
www.intechopen.com

InTech China
Unit 405, Office Block, Hotel Equatorial Shanghai
No.65, Yan An Road (West), Shanghai, 200040, China
中国上海市延安西路65号上海国际贵都大饭店办公楼405单元
Phone: +86-21-62489820
Fax: +86-21-62489821